PRELIMINARY DEVELOPMENT OF CUTTING TOOLS WITH FUNCTIONALLY GRADED MATERIALS

Marcelo Bertolete Carneiro, bertolete@hotmail.com
Izabel Fernanda Machado, machadoi@usp.br
Department of Mechatronics Engineering and Mechanical Systems, Polytechnic School, University of São Paulo, Zip code 05508-900

Daniel Rodrigues, daniel@brats.com.br
BRATS – Filtros Sinterizados e Pós Metálicos, Zip code 07750-000

Abstract. *There is a great interest in making parts with functionally graded materials (FGM), in order to improve the properties associated. Thus the aim is to present the viability of manufacturing ceramic-metal cutting tools in FGM with stepped gradient in at least two phases. Preliminary experiments were performed with Al_2O_3-ZrO_2, Al_2O_3-TiC and WC-Co powders. The samples were sintered in a Dr. Sinter-Syntex machine of Spark Plasma Sintering (SPS), which allows heating rate greater than that of conventional sintering techniques, with the advantage of lower temperature, time and energy consumption. The results showed that mixed ceramic plus cemented carbide did not present macroscopic defects (cracks) on the interface, while pure ceramic, intermediate phase, plus cemented carbide, still showed cracks, mainly in ceramic parts.*

Keywords*: functionally gradient materials, cutting tools, spark plasma sintering*

1. INTRODUCTION

Functionally Gradient Material (FGM) is a novel concept for using innovative properties and/or functions that can not be achieved by conventional homogeneous materials. In its simplest structure, it consists of one material on one side, a second material on the other, and an intermediate layer the structure, composition and morphology of which vary smoothly from one material to the other (Kawasaki and Watanabe, 1997). Mott and Evans (1999) extend the concept and describe FGM as a two-phase material, the volume fraction of the second phase of which increases across the thickness of the material in a gradient which may be continuous or stepwise. Continuous gradients have smooth transitional gradient across the microstructure, whereas stepped gradients are characterized by abrupt changes in composition arising from limitations of the manufacturing route.

This principle provides a solution to many advanced applications in which two or more materials with distinct properties are required to be used jointly. FGM has drawn the attention of researchers from all over the world and a wide range of applications has been reported as ceramics-metal and its ballistic performance, mechanical and thermal properties improvement, biomedical, optical, energy areas and recently in piezoelectricity (Ma and Tan, 2001). Thus, it is evident that graded materials hold the key for many applications, which includes structural materials that can endure high temperature exposure with wear resistance (Kawasaki and Watanabe, 1997). Cutting tools in machining must resist wear at high temperatures and support cutting process forces (Trent and Wrigth, 2000; Shaw, 2005); hence, a ceramic-metal blend can improve the insert design.

The FGM manufacturing process is one of the most important areas in this research theme and a huge spectrum of processing methods has been reported. These include powder metallurgy (P/M), thermal spray, chemical vapor deposition and combustion synthesis. Among these methods, nevertheless, the powder metallurgy is the one most commonly employed due to its wide range of composition and microstructure control and shape forming capability (Ma and Tan, 2001). Some researches, such as Mott and Evans (1999), make ceramic FGM through a sophisticated technique in which complex samples are constructed from droplets of ceramic ink jet printing by an incremental building process. This method allows controlling not only the shape but also the microstructure of ceramic parts, via computer interface. It orders composites in which the profile of a functional gradient (continuous or stepwise) is preset by a computer.

However, the choice of the sintering temperature is not trivial for ceramic-metal mixtures. Generally, metal sinters at a lower temperature than ceramic and the maximum temperature is fixed by melting temperature or grain size growth issues of the metallic powder. This often leads to material partially densified; to improve it, sintering can be aided by applying a pressure, uniaxially between punches or isostatically. Recently, the spark plasma sintering (SPS) has gained interest for densifying heterogeneous powder mixture (Gillia and Caillens, 2010). Tokita (2000) states that the SPS system offers many advantages over conventional systems (hot press – HP, hot isostatic pressing – HIP or atmospheric furnaces), because it is conducted at lower temperatures, with shorter operation, more accurate control of energy, higher sintering velocity and reproducibility, due to large spark pulse current direct on the graphite die and powder under uniaxial compression, that promote the fast heating of powder particles by Joule effect and/or heat transfer. He also says

this method is appropriate for manufacturing functionally grade materials (FGM), intermetallic compounds, fiber reinforced ceramics (FRC), metal matrix composites (MMC) and nanocrystalline materials.

The aim of this work is to present the results of sintering dynamic by SPS of stepwise FGM samples and interface micrographs as a preliminary development of manufacturing viable ceramic-metal cutting tools.

2. EXPERIMENTAL PROCEDURE

The materials used were powders of cemented carbide (WC-Co) and two types of aluminum-oxide (alumina) based ceramics, pure or white (Al_2O_3-ZrO_2) and mixed or black (Al_2O_3-TiC). Figure 1 shows EDS analysis of the powders.

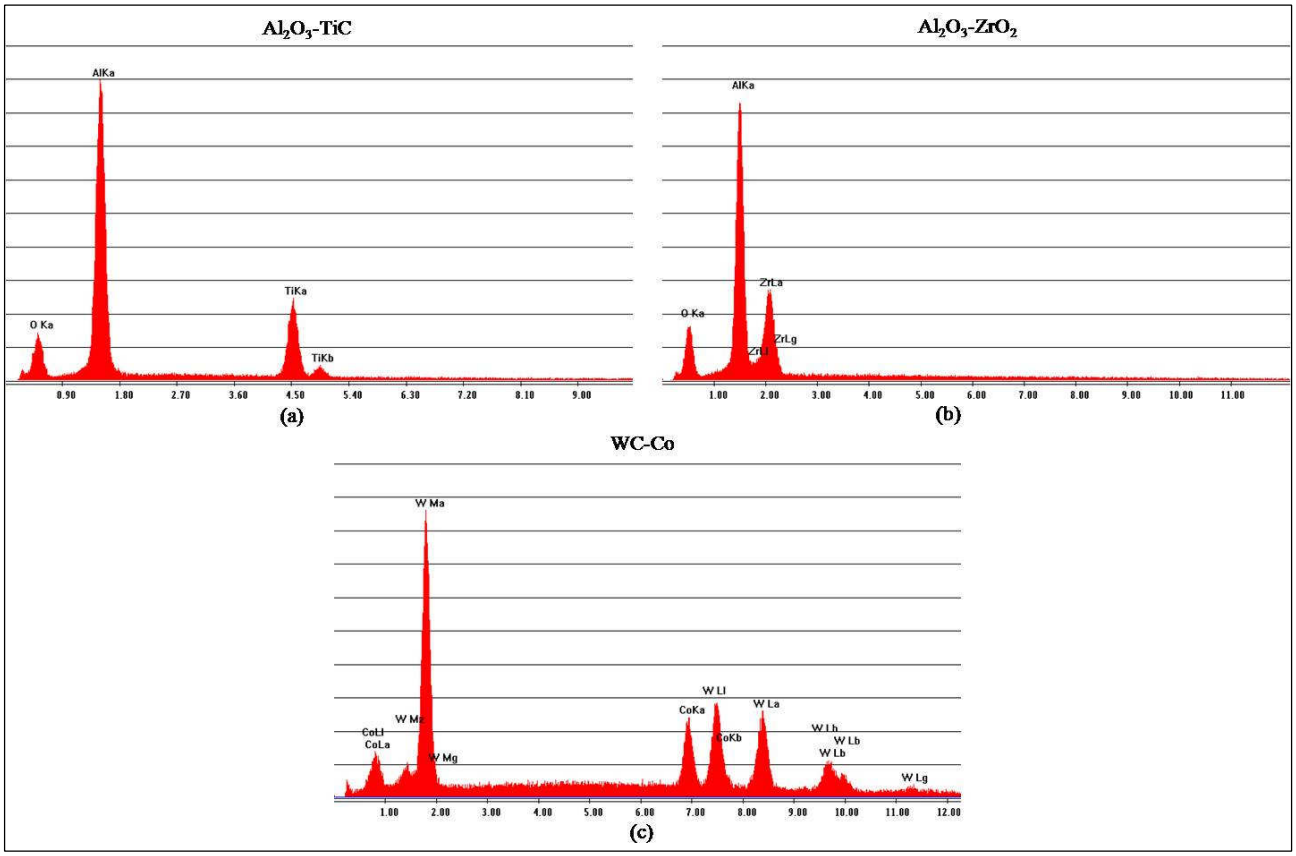

Figure 1. EDS analysis of powders experimented.

Figure 2 presents powder samples in the form of aggregates particles registered in SEM 2000x. The particle size of Al_2O_3-TiC is 0.4 µm, Al_2O_3-ZrO_2 is 0.5 µm and WC-Co is 4 µm.

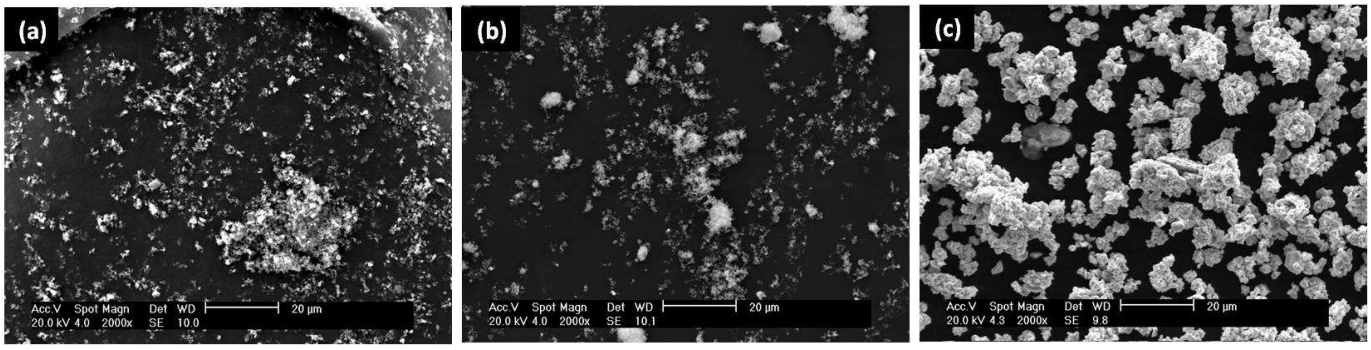

Figure 2. Powders: (a) Al_2O_3-TiC; (b) Al_2O_3-ZrO_2 and (c) WC-Co.

The samples were sintered in a SPS 1050 Dr. Sinter® Syntex Inc. spark plasma sintering machine, which applied an uniaxial pressure on loose powders into a graphite die during heat treatment. The process was performed in vacuum lesser than 10 Pa and the current DC pulsed pattern used was 12 pulses on and 2 pulses off, with each pulse having a

durantion of about 3 ms. The die had external diameter of 50 mm and a 20 mm inner hole; the sintered form obtained was a disc. In addition, in the die wall and interface between punches and powder, a graphite sheet (PermaFoil PF40R2) was used to facilitate the extraction of a specimen after sintering, see Fig. 3.

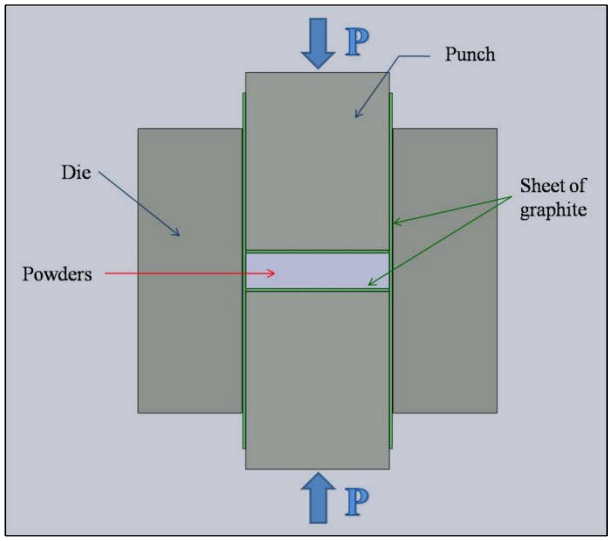

Figure 3: Longitudinal section of die assembly.

Table 1 shows the exploratory tests to verify the viability of manufacturing ceramic-metal cutting tools in FGM with stepwise gradient with at least two phases. Tests 1 to 3 were performed in a single layer for characterizing the sintering dynamic of each powder separately, tests 4 to 6 in two layers and test 7 in three layers, in which the mixture of Al_2O_3-ZrO_2+WC-Co realized in crucible was introduced as an intermediate layer. The process parameters indicate pressure, temperature and holding time of sintering, respectively.

Table 1. Exploratory viability tests.

Tests	Description	Process Parameters
1	Al_2O_3-TiC (single layer)	60 MPa; 1300ºC and 6 min
2	Al_2O_3-ZrO_2 (single layer)	60 MPa; 1300ºC and 6 min
3	WC-Co (single layer)	60 MPa; 1200ºC and 1 min
4	Al_2O_3-TiC+WC-Co (2 layers)	50 MPa; 1140ºC and 2 min
5	Al_2O_3-ZrO_2+WC-Co (2 layers)	50 MPa; 1300ºC and 2 min
6	Al_2O_3-TiC+WC-Co (2 layers)	45 MPa; 1200ºC and 6 min
7	Al_2O_3-ZrO_2+WC-Co (3 layers)	45 MPa; 1200ºC and 6 min

The sintering dynamics, which includes mainly displacement rate, temperature and pressure, was recorded by the data acquisition system sensors of the SPS machine in time function (dilatometer, pyrometer and load cell) for a better process understanding. Displacement rate monitoring is important because it provides substantial insight about microscopic changes during sintering; the temperature supplies energy, since the process is thermally activated and at last pressure rises contact points among particles and densification rate (Kang, 2005; German, 1996).

Finally, compacts micrographs were made in an optical microscope (OM) Olympus BX60M with CCD camera coupled and scanning electron microscope (SEM) Philips XL30, with magnification of samples cross-section of 50x and 100, 500, 1000 and 2000x, respectively.

3. RESULTS AND DISCUSSION

The results of sintering dynamics and compacts micrographs are presented in accordance with Tab. 1. The viability for manufacturing cutting tools in FGM is related with the presence of microstructural defects (crack and porosity) in sintered samples. Thus, sample images are shown in cross-section, in general not polished, making possible to distinguish blade feed marks and cracks; nevertheless, the porosity will not be discussed.

Figure 4 shows the results of the sintering process monitoring of Al_2O_3-TiC (single layer), in treatment conditions of 60 MPa, 1300°C and 6 minutes of holding time (Test 1). A circular highlighted region is observed in the displacement rate curve which refers to particles rearrangement due to pressure increase. Peak 1 in this curve occurs at the coordinate (Time;Temperature) of 18.75 min and 1053°C and evidences microscopic change, not necessarily polymorphism or allotropy, with large displacement, i.e. sintering. Peak 2 at 21.08 min and 1290°C also indicates sintering. Peak 3 is the final moment of the thermal cycle and pressure removal.

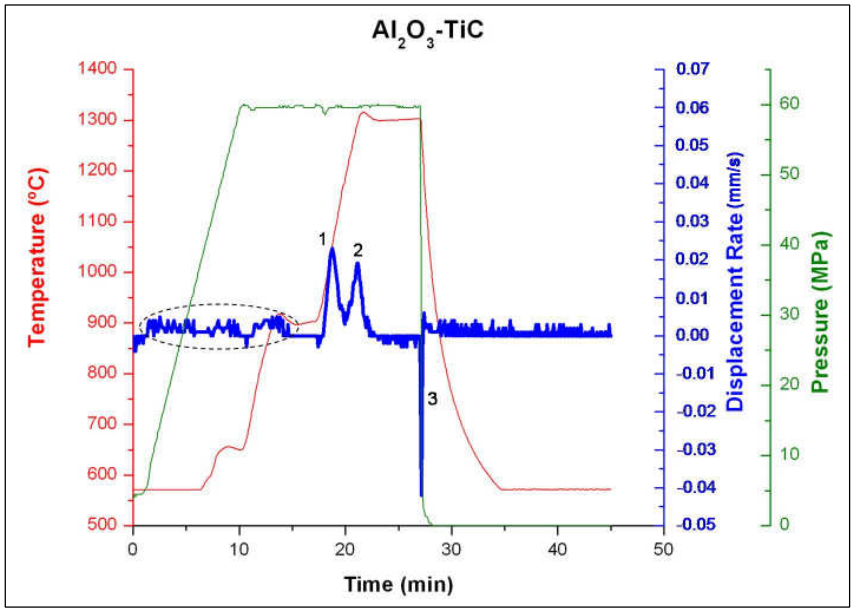

Figure 4. Sintering of Al_2O_3-TiC (60 MPa, 1300°C and 6 min)

Figure 5 shows micrographs of mixed ceramic (Al_2O_3-TiC) processed in a single layer; no cracks, only feed marks enhanced, are observed.

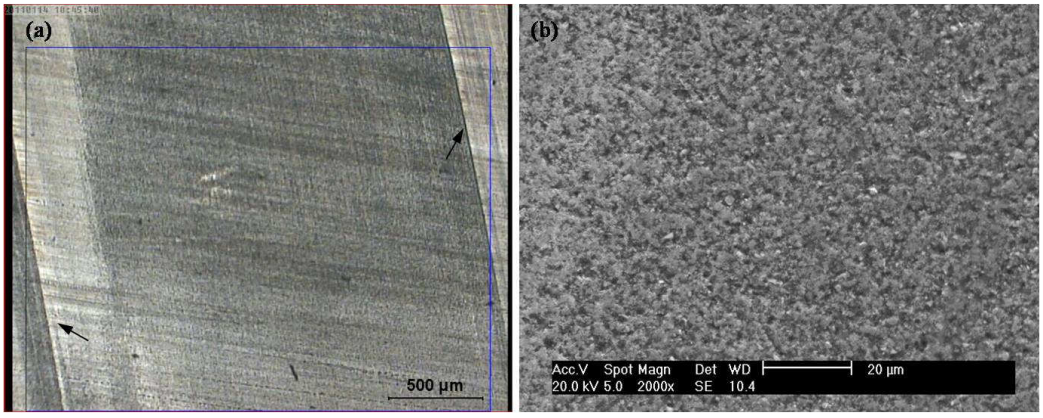

Figure 5. Al_2O_3-TiC (60 MPa, 1300ºC and 6 min): (a) OM 50x the arrows indicate feed marks; (b) SEM 2000x

Figure 6 presents the results of Al_2O_3-ZrO_2 sintering (single layer), on conditions of 60 MPa, 1300ºC and 6 minutes of holding time (Test 2). The circular region in the displacement rate refers to particles rearrangement, because of pressure action. Peaks 1 and 2 show large changes in displacement, which denotes sintering, and they occur at 18.83 min and 1069°C and 21.08 min and 1289°C, respectively. Peak 3 is the end of the thermal treatment.

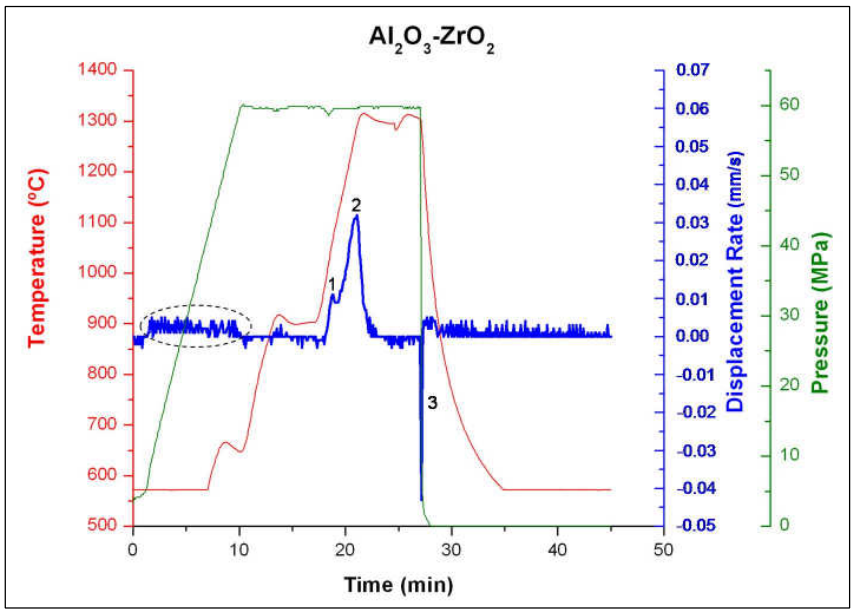

Figure 6. Sintering of Al_2O_3-ZrO_2 (60 MPa, 1300°C and 6 min)

In Figure 7 also no cracks are verified on pure ceramic (Al_2O_3-ZrO_2) treated singly.

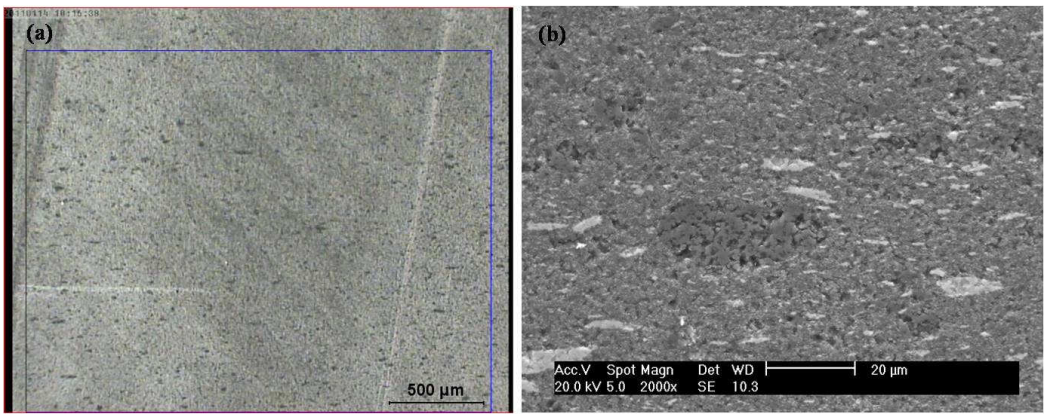

Figure 7. Al_2O_3-ZrO_2 (60 MPa, 1300ºC and 6 min): (a) OM 50x; (b) SEM 2000x

In Figure 8, the process results for WC-Co (Test 3) are shown in conditions of 60 MPa, 1200°C and 1 minute of holding time; in this test, a viscous flow of material out of the die (solubility WC in Co liquid phase and pressure pouring) was observed. The circular region highlighted in the displacement rate curve also refers to a large rearrangement of particles, due to pressure application; however, in a loading cycle a little different from previous tests. Peak 1 indicates sintering at 10.3 min and 1001°C. Peak 2 refers to the moment at which material leakage out of the die occurs at 12.67 min and 1200°C.

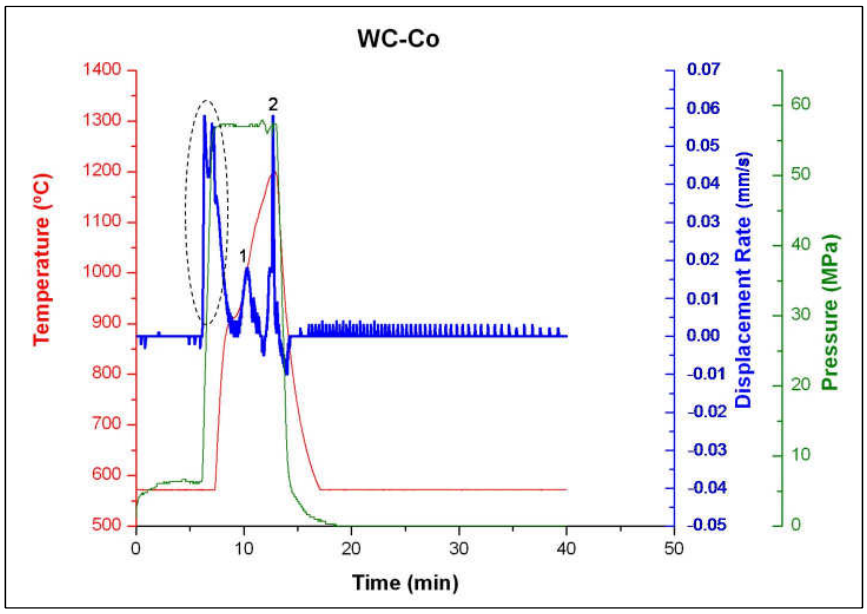

Figure 8. Sintering of WC-Co (60 MPa, 1200°C and 1 min)

Owing to material viscous flow out of the die, the assembly die-workpiece-punches get linked, thus the sample was lost and its image could not be presented.

The results of sintered samples monitoring with stepwise FGM characteristic are presented as follows.

Figure 9 shows the sintering of Al_2O_3-TiC+WC-Co (Test 4) in conditions of 50 MPa, 1140°C and 2 minutes. The circular region highlighted in displacement rate curve refers to particles rearrangement due to pressure increase. Peak 1 indicates the possible sintering of cemented carbide at 14.72 min and 1022°C, as compared with peak 1 (10.3 min and 1001°C) of Test 3, Fig. 8; due to lesser pressure and temperature conditions (driving force), this peak occurs with a little higher temperature. Peak 2 refers to mixed ceramic sintering at 18.15 min and 1142°C, which can be compared with peak 1 (18.75 min and 1053°C) of Test 1 presented in Fig. 4, for the same reason as before, the peak occurs with a little higher energy level.

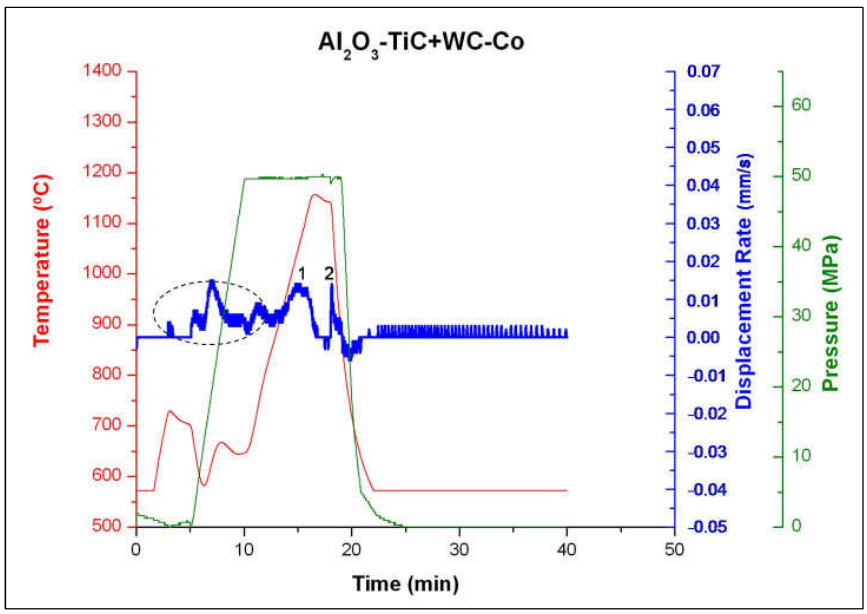

Figure 9. Sintering of Al_2O_3-TiC+WC-Co (50 MPa, 1140°C and 2 min)

Figure 10 presents an image of a polished sample of stepwise FGM. No cracks are observed in the interface between mixed ceramic and cemented carbide, probably due to better conditions for mass transport mechanisms involved and higher toughness of this alumina.

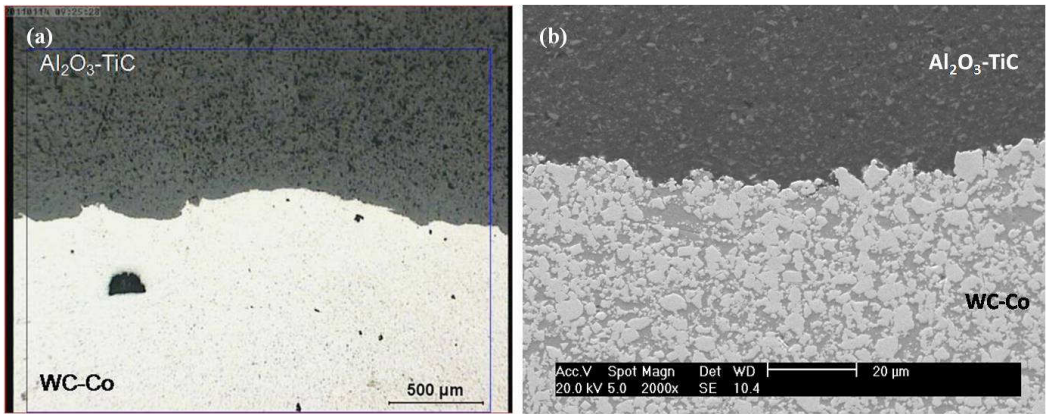

Figure 10. Al_2O_3-TiC+WC-Co (50 MPa, 1140°C and 2 min): (a) OM 50x; (b) SEM 2000x

The sintering of Al_2O_3-ZrO_2+WC-Co at 50 MPa, 1300°C and 2 minutes – Test 5 – is presented in Fig. 11. The circular region in the displacement rate is characterized by particles rearrangement due to uniaxial load action. The rectangular region presents a constant displacement rate which occurs in a period of 10.17 at 11.67 min with temperature between 746 and 918°C; from this range, it is difficult to define the sintering point of the cemented carbide. Peak 1 corresponds to the coordinate 12.75 min and 1040°C may be related to WC-Co, as compared with the results presented in Fig. 8 (10.3 min and 1001°C) Test 3 and Fig. 9 (14.72 min and 1022°C) Test 4. Peak 2 is closer to being characterized as white ceramic sintering point, since it occurs at 13.58 min and 1127°C with a little higher energy level than that in Fig. 6 (18.83 min and 1069°C) Test 2, justified by lesser level of pressure applied. Peak 3 at 14.67 min and 1232°C represents the leaking of cemented carbide out of the die, characterizing viscous flow, as the point presented in Fig. 8 at 12.67 min and 1200°C. Peak 4 refers to the second peak of Al_2O_3-ZrO_2 sintering, which occurred at 17.17 min and 1304°C and was shown in Fig. 6 at 21.08 min and 1289°C.

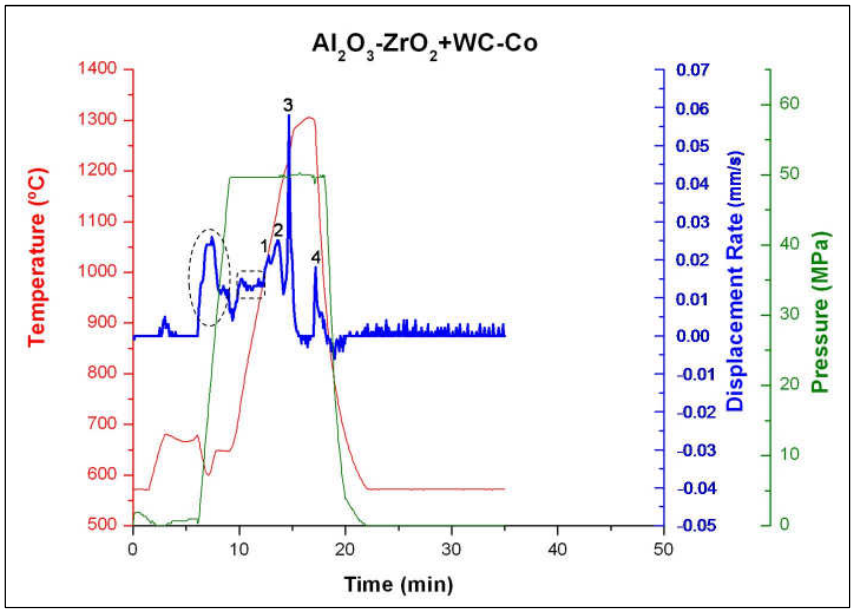

Figure 11. Sintering of Al_2O_3-ZrO_2+WC-Co (50 MPa, 1300°C and 2 min)

In Figure 12, feed marks and cracks are observed in the interface and mainly in the ceramic phase, which promoted the detachment between phases. The presence of these great cracks can be due to small holding time (2 minutes) which did not permit the full densification or absence of the mix intermediate phase of the two powders to minimize the difference in thermal expansion coefficient.

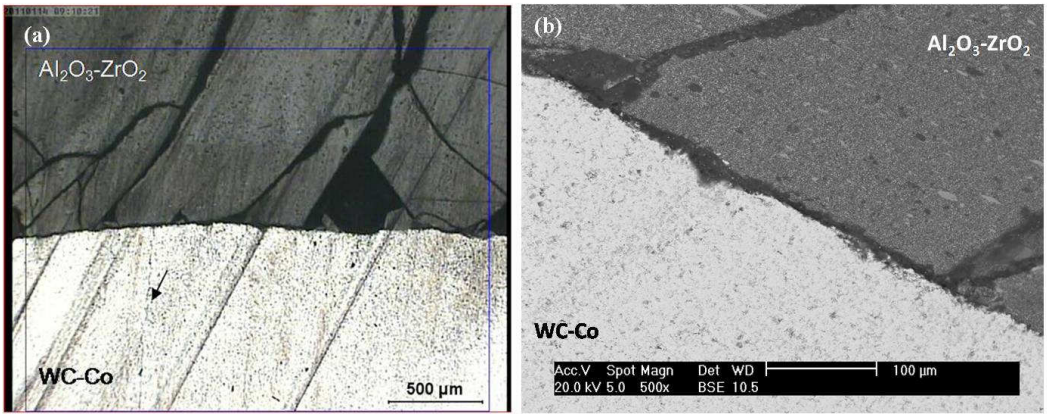

Figure 12. Al_2O_3-ZrO_2+WC-Co (50 MPa, 1300°C and 2 min): (a) OM 50x the arrow indicates a crack in WC-Co layer; (b) SEM 500x

Figure 13 shows the sintering of Al_2O_3-TiC+WC-Co at 45 MPa, 1200°C and 6 minutes of holding time; the maximum temperature reached was observed to be 1099°C. The circular region refers to the accommodation of the powder particles, due to pressure increase. Peak 1 refers to the cemented carbide sintering which occurred at this cycle stage at 52 MPa at a 13.5 min time and temperature of 941°C, an inferior energy level than that presented in Fig. 8 (10.3 min and 1001°C) of Test 3. Peak 2 at 45 MPa, 19 min and 1089°C refers to black ceramic sintering; a similar point is shown in Fig. 4 (18.75 min and 1053°C), Test 1. In peak 3, the process ends with immediate load removal.

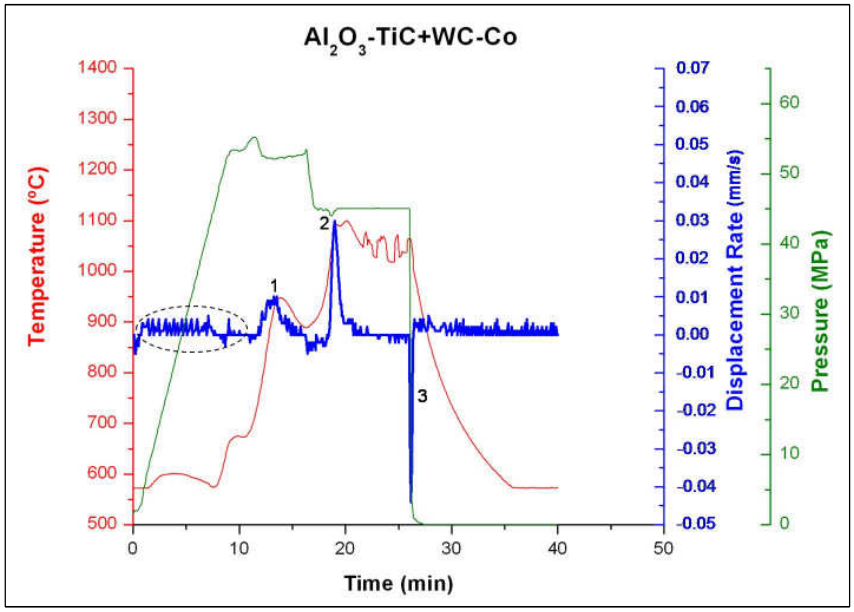

Figure 13. Sintering of Al_2O_3-TiC+WC-Co (45 MPa, 1200°C and 6 min)

Figure 14 shows feed marks, oxidation spot (highlight) due to friction and heat generation between blade and sample, besides absence of cracks in the layer interface.

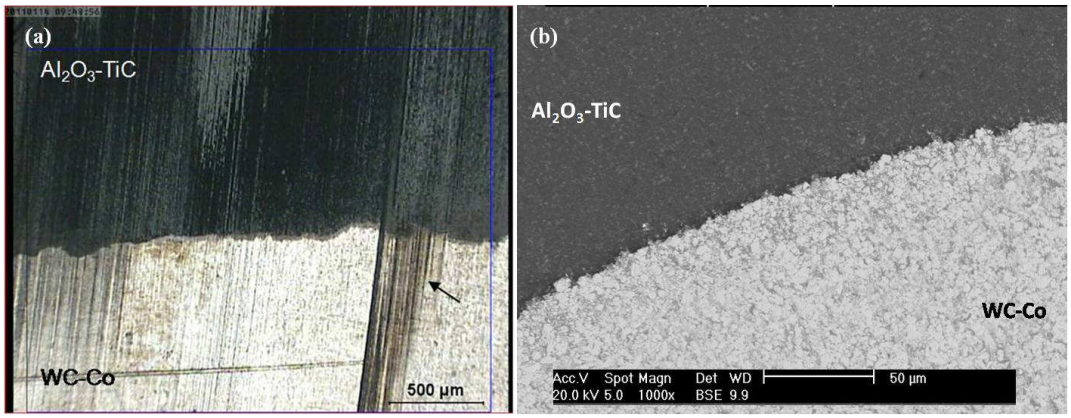

Figure 14. Al_2O_3-TiC+WC-Co (45 MPa, 1200°C and 6 min): (a) OM 50x the arrow indicates oxidation spot; (b) SEM 1000x

Figure 15 shows the processing of Al_2O_3-ZrO_2+WC-Co at 45 MPa, 1200°C and 6 minutes; cemented carbide was observed to leak out of the die. The circular region highlighted in the displacement rate represents the powder particles accommodation, due to pressure action. The rectangular region suggests cemented carbide sintering, which largely occurs at 54 MPa with a time range between 11.75 and 18.33 min and temperature of 751 to 990°C, respectively. Peak 1 refers to white ceramic sintering at 45 MPa with coordinate 19.17 min and 1112°C, a similar point to that shown in Fig. 6 (18.83 min and 1069°C), Test 2. In peak 2, viscous flow of cemented carbide occurred at 20.5 min and 1243°C, a similar condition is presented in Fig. 8 (12.67 min and 1200°C), Test 3. In both peaks, the inferior pressure influences a higher energy level. Finally, peak 3 represents the end of treatment and load removal.

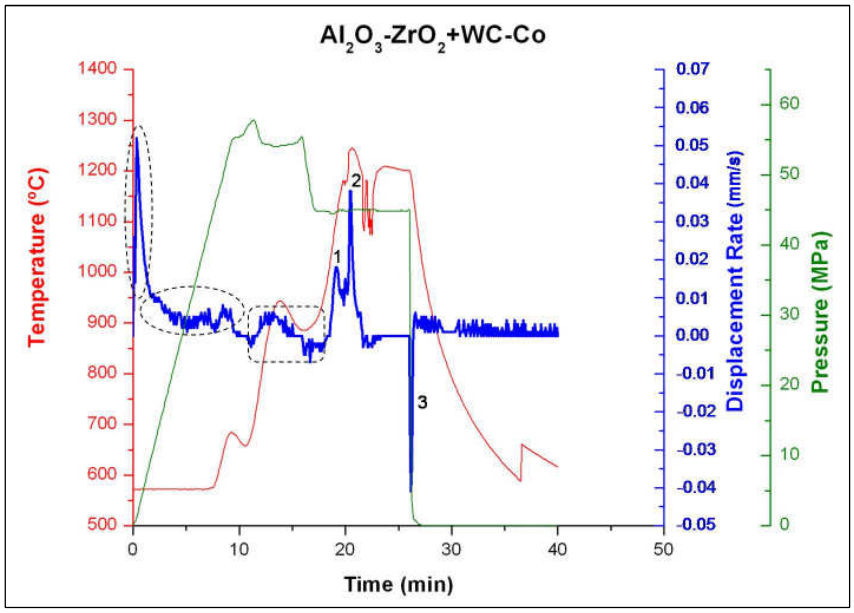

Figure 15. Sintering of Al_2O_3-ZrO_2+WC-Co (45 MPa, 1200°C and 6 min)

Figure 16 presents an image of stepwise FGM sample with three layers. More cracks are observed at the ceramic layer than at the intermediate one, yet without material detachment; besides, cracks are not verified on the cemented carbide. The presence of cracks in this alumina type can be due to its lower toughness, mainly owing to shrinkage stress.

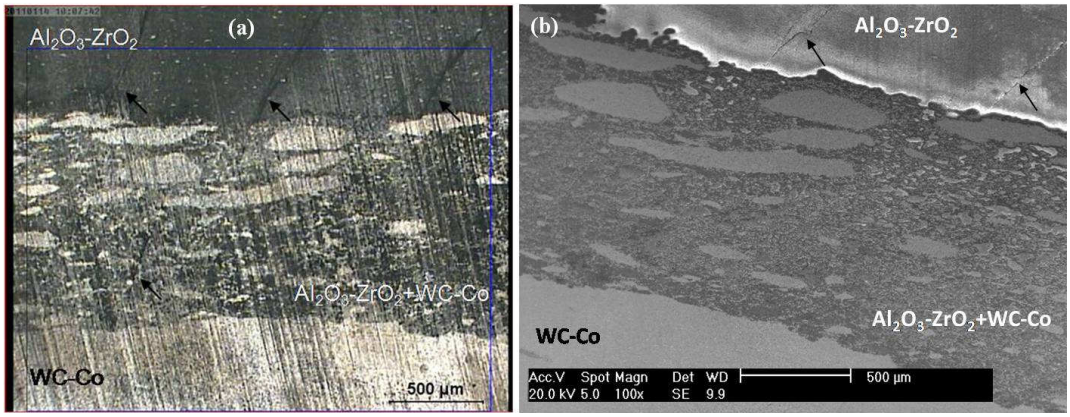

Figure 16. Al_2O_3-ZrO_2+WC-Co (45 MPa, 1200°C and 6 min): (a) OM 50x; (b) SEM 100x. In both images the arrows indicate cracks

4. CONCLUSION

Mechanical components with non-uniform properties are interesting for development of new products and applications, mainly if passing from material with hard (brittle) behavior to more ductile one in a single integrated component.

Through the sintering dynamic monitoring, exploratory tests allowed relating the coordinates which evidenced the sintering of powders and the viscous flow of cemented carbide. Also, it was possible verify the viability of graded material manufacturing between mixed ceramic and cemented carbide, in both process conditions tested; nevertheless, the mixture with white ceramic needs to be improved, because cracks kept occurring, mainly in the ceramic part probably due to shrinkage stress.

5. ACKNOWLEGMENTS

The research counted on support from FAPESP (process 2010/0683-2 and 2010/01073-3), CAPES, CNPq (process 472145/2010-0), PETROBRAS and from the Laboratory of Electronic Microscopy and Atomic Force – USP.

6. REFERENCES

Gillia O., Caillens B., 2010, “Fabrication of a material with composition gradient for metal/ceramic assembly”, Powder Technol., doi:10.1016/j.powtec.2010.08.029

Kawasaki, A. and Watanabe, R., 1997, “Concept and P/M Fabrication of Functionally Gradient Materials”, Ceram. International, 23, pp 79-83.

Ma, J. and Tan, G.E.B., 2001, “Processing and Characterization of Metal-Ceramics Functionally Gradient Materials”, J. Mat. Proc. Technology, 113, pp 446-449.

Mott, M. and Evans, J.R.G., 1999, “Zirconia/Alumina Functionally Graded Material Made by Ceramic Ink Jet Printing”, M. Sc. Engineering A, 271, pp 344-352.

Shaw, M. C., 2005, “Metal Cutting Principles”, 2nd Edition, Oxford University Press, 651 p.

Tokita, M., 2000, “Mechanism of Spark Plasma Sintering”, Proceedings of 2000 Powder Metallurgy World Congress, Kyoto, Japan, pp 729-732.

Trent, E. M. and Wright, P. K., 2000, “Metal Cutting”. 4th edition. Butterworth-Heinemann, 446p.

7. RESPONSIBILITY NOTICE

The authors are the only responsible for the printed material included in this paper.